Available at
www.ElsevierComputerScience.com
POWERED BY SCIENCE DIRECT®
Signal Processing 85 (2005) 581–590
SIGNAL PROCESSING
www.elsevier.com/locate/sigpro

Extrapolated impulse response filter and its application in the synthesis of digital filters using the frequency-response masking technique

Y.J. Yu[a,*], K.L. Teo[b], Y.C. Lim[c], G.H. Zhao[b,d]

[a]*Temasek Laboratories, Research Techno Plaze, Nanyang Technological University, Singapore 639798, Singapore*
[b]*Department of Applied Mathematics, The Hong Kong Polytechnic University, Hong Kong, PR China*
[c]*School of Electrical and Electronics Engineering, Nanyang Technological University, Singapore 639798, Singapore*
[d]*Department of Applied Mathematics, Dalian University of Technology, Liaoning 116024, PR China*

Received 25 August 2003; received in revised form 20 July 2004

Abstract

Techniques based on the frequency-response masking (FRM) approach are known to be highly effective for reducing the number of multipliers and adders in linear-phase finite-impulse response (FIR) filters. The basic FRM structure comprises a band-edge shaping filter and two masking filters. It is observed that the impulse response of the band-edge shaping filter of an FRM structure exhibits a quasi-periodic property. Previous study showed that lowpass or highpass digital FIR filters, whose impulse responses are quasi-periodic, can be synthesized using extrapolated impulse response technique, which leads to structure with much reduced arithmetic complexity. In this paper, an implementation of the extrapolated impulse response filter is presented. An FRM technique incorporating extrapolated impulse response band-edge shaping filter is introduced. An iterative optimization procedure is proposed to design the FRM sub-filters. It is demonstrated using an example taken from the literature that our new technique produces a saving of over 20% in the number of multipliers used.
© 2004 Elsevier B.V. All rights reserved.

Keywords: Extrapolated impulse response; Frequency-response masking

1. Introduction

Frequency-response masking (FRM) technique [1–7,9–14] produces a filter network, as shown in Fig. 1, which comprises a band-edge shaping filter, $F(z^L)$, and two masking filters, $G_1(z)$ and $G_2(z)$, to synthesize narrow transition band linear phase

*Corresponding author. Tel.: +65 6790 6674; fax: +65 6790 0215.
E-mail address: eleyuyj@pmail.ntu.edu.sg (Y.J. Yu).

0165-1684/$ - see front matter © 2004 Elsevier B.V. All rights reserved.
doi:10.1016/j.sigpro.2004.11.003

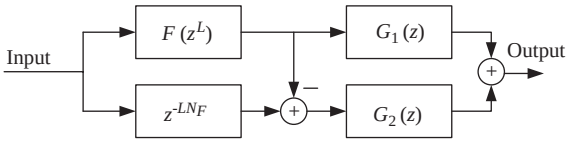

Fig. 1. A filter synthesized using the FRM technique.

digital FIR filters. $F(z^L)$ is obtained by replacing each delay element of a prototype filter, $F(z)$, by L delay elements and therefore has very sharp transition bands and very low arithmetic complexity. However, if the desired FIR filter has an extremely narrow transition band, the order of the band-edge shaping filter may still be high when a single-stage FRM approach is used.

It is interesting to note that the impulse response of the band-edge shaping filter, $f(n)$ for $|n| \leqslant N_F$, where $2N_F + 1$ is the filter length, shows a quasi-periodic property. In view of this property, an FRM technique incorporating extrapolated impulse response band-edge shaping filter is introduced in this paper.

The extrapolated impulse response approach was proposed in [8] to synthesize lowpass and highpass filters with reduced complexity by making use of the correlation between blocks of impulse response samples. In this approach, smaller side lobes of impulse response samples are approximated as scaled versions of larger ones so as to extrapolate the filter length. Thus, the hardware complexity of the filter is reduced.

The rest of the paper is organized as follows. Section 2 reviews the extrapolated impulse response technique. An implementation of the extrapolated impulse response structure by exploiting the coefficient symmetry is proposed. Section 3 briefly reviews the FRM technique. In Section 4, the extrapolated impulse response approach is incorporated into the FRM technique to further reduce the complexity of the band-edge shaping filter. An optimization procedure is proposed to iteratively optimize the extrapolated band-edge shaping filter and the masking filters. Section 5 discusses the choice of parameters which play important roles in the optimization procedure. The example in Section 6 shows that the numbers of adders and multipliers of the resulting filter designed using our technique are less than 80% of those obtained earlier in [11].

2. The extrapolated impulse response

This section reviews the extrapolated impulse response approach for synthesizing FIR filters. A realization structure for the extrapolated impulse response filter by making use of the coefficient symmetry is also presented.

A typical impulse response sequence, $h(n)$, of an FIR filter is quasi-periodic, consisting of a center lobe with the largest magnitude and side lobes with decreasing magnitude away from the center, as shown in Fig. 2. The zero phase transfer function of $h(n)$ is

$$H(z) = h(0) + \sum_{n=1}^{N} h(n)(z^n + z^{-n}). \tag{1}$$

Assume that the impulse response has lobes at $n = k_0 + 1 = M + 1$ through $n = k_1, n = k_1 + 1$ through $n = k_2, \ldots$, and $n = k_{p-1} + 1$ through $n = k_p = N$. $H(z)$ may be rewritten as

$$\begin{aligned} H(z) = h(0) &+ \sum_{n=1}^{M} h(n)(z^n + z^{-n}) \\ &+ \sum_{n=k_0+1}^{k_1} h(n)(z^n + z^{-n}) \\ &+ \sum_{n=k_1+1}^{k_2} h(n)(z^n + z^{-n}) \\ &+ \cdots + \sum_{n=k_{p-1}+1}^{N} h(n)(z^n + z^{-n}). \end{aligned} \tag{2}$$

The durations of side lobes, $k_1 - k_0, k_2 - k_1, \ldots$, and $k_p - k_{p-1}$, may or may not be all equal. For any two side lobes having the same number of impulse response samples, the smaller lobe may be approximated by a scaled version of the larger one. For example, if $k_{m+1} - k_m = k_{l+1} - k_l = d$, then

$$h(k_m + n) = \alpha h(k_l + n) \quad \text{for } n = 1, 2, \ldots, d, \tag{3}$$

where α is an approximate scaling factor. Thus, for the impulse response shown in Fig. 2, the 5th side

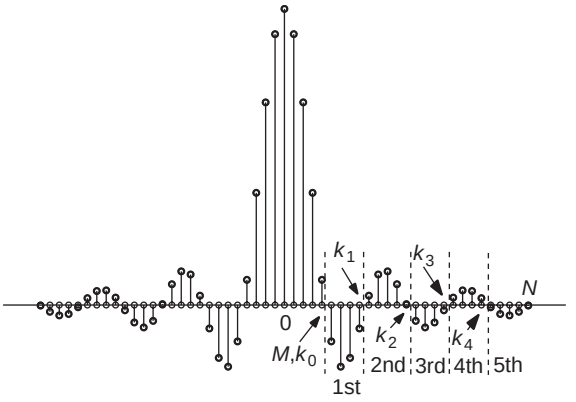

Fig. 2. A typical impulse response sequence of a lowpass filter.

lobe can be approximated as a scaled version of the 2nd side lobe, and the 3rd and 4th side lobes can be approximated as scaled versions of the 1st side lobe.

For expository convenience, we assume that all the side lobes are of the same duration, d. Extensions to other cases are simple and straightforward. For the case considered in this paper, (2) may be rewritten as

$$H(z) = h(0) + \sum_{n=1}^{M} h(n)(z^{n} + z^{-n}) + \sum_{r=0}^{R}\sum_{m=1}^{d} h(M+m+rd) \times \left(z^{M+m+rd} + z^{-(M+m+rd)}\right), \quad (4)$$

where $R+1$ is the number of lobes. If the lobes for $r \geqslant 1$ are approximated as scaled versions of the lobe for $r = 0$, $H(z)$ can be approximated by

$$H(z) \approx \hat{H}(z) = h(0) + \sum_{n=1}^{M} h(n)(z^{n} + z^{-n}) + \sum_{m=1}^{d} h(M+m)\sum_{r=0}^{R} \alpha_r \times \left(z^{M+m+rd} + z^{-(M+m+rd)}\right), \quad (5)$$

where α_r is the rth scaling factor and $\alpha_0 = 1$.

The frequency response $\hat{H}(e^{j\omega})$ of the extrapolated impulse response filter is given by

$$\hat{H}(e^{j\omega}) = h(0) + 2\sum_{n=1}^{M} h(n)\cos(n\omega) + 2\sum_{m=1}^{d} h(M+m)\sum_{r=0}^{R} \alpha_r \times \cos((M+m+rd)\omega). \quad (6)$$

In remaining part of this section, a realization structure for the extrapolated impulse response filter by making use of the coefficient symmetry is presented.

Eq. (5) may be realized in hardware in three separate sections. The center section, which consists of the first two terms, is the well-known direct form FIR filter. Terms associated with $\sum \alpha_r z^{-(M+m+rd)}$ can be realized using the structure shown in Fig. 3(a) and terms associated with $\sum \alpha_r z^{M+m+rd}$ can be realized using the structure shown in Fig. 3(b). Fig. 3(c) shows a realization of the transfer function

$$H(z) = h(0) + h(1)(z + z^{-1}) + h(2)(z^{2} + z^{-2}) + \sum_{m=1}^{2} h(2+m)\sum_{r=0}^{2} \alpha_r \times \left(z^{2+m+2r} + z^{-(2+m+2r)}\right). \quad (7)$$

The structure shown in Fig. 3 is a transposed form of the structure proposed in [8]. The advantage of this structure is that the coefficient symmetry can be exploited leading to a saving of d multipliers. An additional advantage of this structure is that there is a saving of $Rd - d + 1$ delay elements when compared with the structure proposed in [8].

3. Frequency-response masking technique

In FRM technique, the overall linear-phase FIR filter transfer function is constructed as [6,7,12]

$$H(z) = F(z^{L})G_1(z) + [z^{-LN_F} - F(z^{L})]G_2(z), \quad (8)$$

where $F(z)$ is the band-edge shaping filter with length $2N_F + 1$, whereas $G_1(z)$ and $G_2(z)$ are the masking filters. If $F(z)$ and $z^{-N_F} - F(z)$ form a lowpass–highpass filter pair with edges at θ and ϕ,

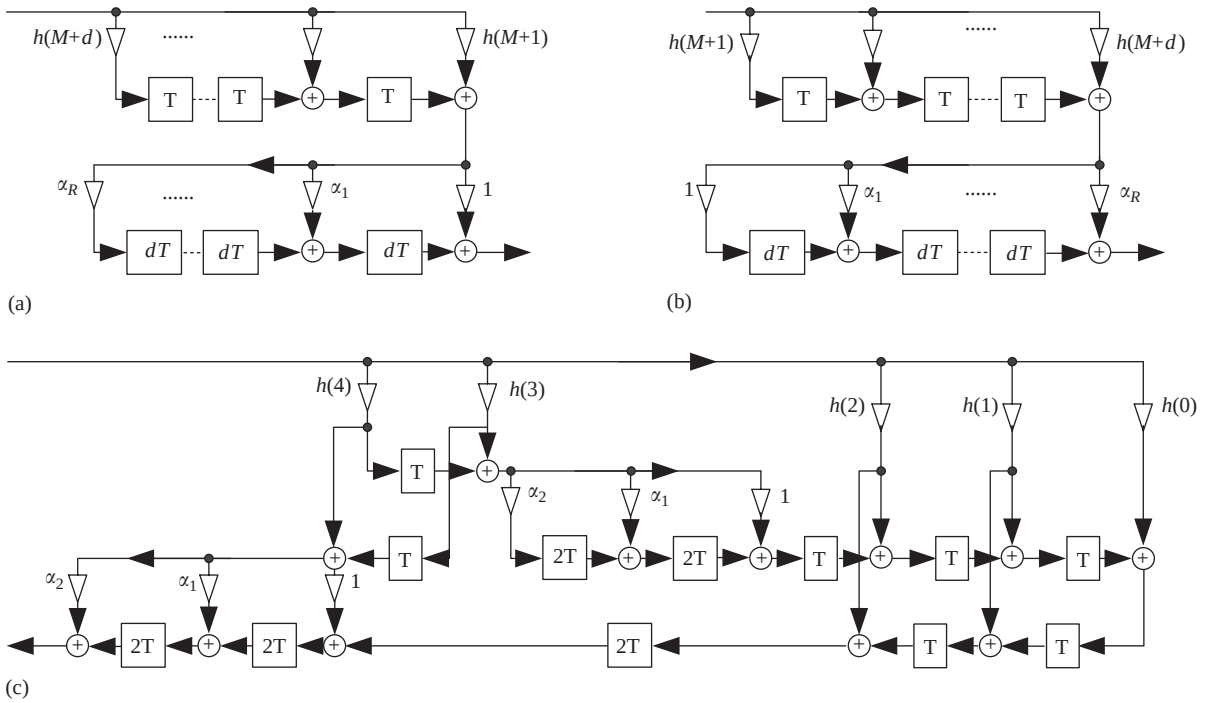

Fig. 3. Realization structures for the extrapolated impulse response filter by making use of the coefficient symmetry, where T represents a single delay element and dT represents d cascaded delay elements.

then $F(z^L)$ and $z^{-LN_F} - F(z^L)$ provide various transition bands of width of $(\phi - \theta)/L$ that are only $(1/L)$ of that of $F(z)$ and $z^{-N_F} - F(z)$. The role of the masking filters $G_1(z)$ and $G_2(z)$ is to attenuate the unnecessary frequency components of $F(z^L)$ and $z^{-LN_F} - F(z^L)$ in order to achieve the desired overall frequency response [6,7].

For a lowpass overall transfer function $H(z)$ with the passband and stopband edges at ω_p and ω_s, and given L, one of the following two cases (but not both) may yield a set of θ and ϕ satisfying $0 \leqslant \theta < \phi \leqslant \pi$. For Case A, the parameters for the FRM design are [6,7,12]

$$l = \lfloor L\omega_p/(2\pi) \rfloor, \quad \theta = L\omega_p - 2l\pi,$$
$$\phi = L\omega_s - 2l\pi \tag{9}$$

and for Case B, the parameters are

$$l = \lceil L\omega_s/(2\pi) \rceil, \quad \theta = 2l\pi - L\omega_s,$$
$$\phi = 2l\pi - L\omega_p. \tag{10}$$

Here, $\lfloor x \rfloor$ is the largest integer less than or equal to x, and $\lceil x \rceil$ is the smallest integer larger than or equal to x.

4. FRM technique incorporating extrapolated impulse response band-edge shaping filter

It is observed that the impulse response of the band-edge shaping filter, $f(n)$ for $|n| \leqslant N_F$, of an FRM structure exhibits quasi-periodic property. An example of an impulse response sequence $f(14)$ through $f(61)$ is shown in Fig. 4.

In Fig. 4, the impulse response lobes themselves do not show obvious periodic property, but the divided segments as shown in Fig. 4 exhibit quasi-periodic property. In Fig. 4, each segment consists of several lobes. The secondary side segments shown in Fig. 4 are approximate scaled versions of the primary side segment, and thus the extrapolated impulse response technique can be

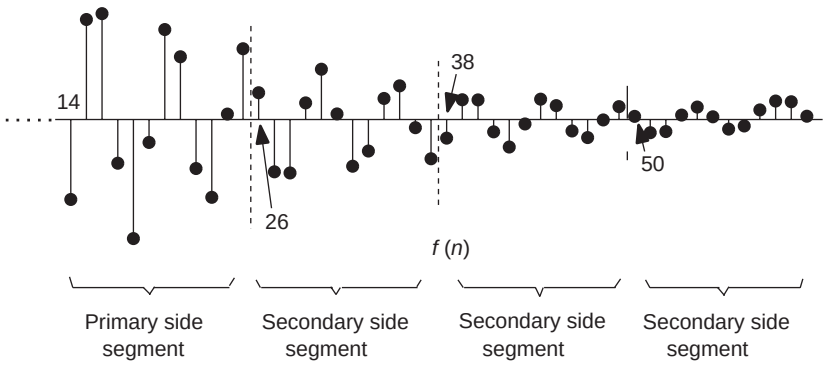

Fig. 4. The impulse response sequence $f(14)$ through $f(61)$ of the band-edge shaping filter $F(z)$, obtained by using the iterative optimization approach [11], shows quasi-periodic property.

incorporated into the FRM technique. As the impulse response is symmetrical in linear phase FIR filters, the impulse responses with negative indexes have a corresponding primary side segment and secondary side segments; these segments are not shown in Fig. 4. The impulse response segment between the two primary side segments is called the center segment.

Our technique starts from an initial design, $F^0(z)$, $G_1^0(z)$ and $G_2^0(z)$, obtained by using the approach proposed in [11], in which the band-edge shaping filter, $F(z^L)$, and the masking filters, $G_1(z)$ and $G_2(z)$, are optimized iteratively; $F(z^L)$ provides the desired overall filter performance on $[\Omega_{p1},\ \Omega_{p2}] \cup [\Omega_{s1},\ \Omega_{s2}]$, whereas $G_1(z)$ and $G_2(z)$ provide the overall filter performance on $[0,\ \Omega_{p1}] \cup [\Omega_{s2},\ \pi]$, where

Case A Design	Case B Design
$\Omega_{p1} = 2l\pi/L,$	$\Omega_{p1} = (2l-1)\pi/L,$
$\Omega_{p2} = (2l\pi+\theta)/L$	$\Omega_{p2} = (2l\pi-\phi)/L$
$\quad = \omega_p,$	$\quad = \omega_p,$
$\Omega_{s1} = (2l\pi+\phi)/L = \omega_s,$	$\Omega_{s1} = (2l\pi-\theta)/L = \omega_s,$
$\Omega_{s2} = (2l+1)\pi/L,$	$\Omega_{s2} = 2l\pi/L.$

(11)

The optimization of the sub-filters of FRM when the band-edge shaping filter is incorporated with the extrapolated impulse response technique can be carried out by embedding another iterative procedure for the design of the band-edge shaping filter. In the embedded iterative procedure, the extrapolated coefficients, $f(n)$ for $n = 0, 1, \ldots, M+d$, and scaling factors, α_r for $r = 1, 2, \ldots, R$ are iteratively optimized and both are taking care of the frequency band of $[\Omega_{p1},\ \Omega_{p2}] \cup [\Omega_{s1},\ \Omega_{s2}]$.

The zero-phase frequency responses of $F(z^L)$, $G_1(z)$ and $G_2(z)$ are denoted as $F(L\omega)$, $G_1(\omega)$ and $G_2(\omega)$. Assuming that the impulse response of $F(z)$ is quasi-periodic from sample $f(M+1)$ through $f(M+(R+1)d)$, and each period is with duration d. The choice of parameters d and M will be discussed in Section 5. The proposed optimization procedure for the design of a lowpass filter, $H(z)$, with passpand and stopband ripples of δ_p and δ_s is as follows:

Step 0: Set counter $p = 0, \varepsilon_G^{(p)} = 0$.

Step 1: Set $p = p + 1$. Determine the parameters of $G_1^{(p)}(\omega)$ and $G_2^{(p)}(\omega)$ to minimize:

$$\varepsilon_G^{(p)} = \max_{\omega\in[0,\Omega_{p1}]\cup[\Omega_{s2},\pi]} |W(\omega)[H_G^{(p)}(\omega) - D(\omega)]|, \quad (12)$$

Here, the first band is the passpand, where $W(\omega)$ and $D(\omega)$ are equal to unity. The second band is the stopband, where $W(\omega)$ is equal to δ_p/δ_s and $D(\omega)$ is equal to zero. In the sequel, the same desired and weighting functions are used. In addition, in (12),

$$H_G^{(p)}(\omega) = F^{(p-1)}(L\omega)G_1^{(p)}(\omega) + \left[1 - F^{(p-1)}(L\omega)\right]G_2^{(p)}(\omega). \quad (13)$$

Step 2: Set counter $q = 0$ and

$$\varepsilon_{\alpha}^{(q-1)} = 0, \varepsilon_{F}^{(q)} = 0,$$
$$\boldsymbol{X}_1^{(q)} = \left[f^{(p-1)}(0), \ldots, f^{(p-1)}(M)\right]^{\mathrm{T}},$$
$$\boldsymbol{X}_2^{(q)} = \left[f^{(p-1)}(M+1), \ldots, f^{(p-1)}(M+d)\right]^{\mathrm{T}},$$
$$\boldsymbol{X}_3^{(q)} = \left[\alpha_0^{(p-1)}, \ldots, \alpha_R^{(p-1)}\right]^{\mathrm{T}}. \tag{14}$$

Step 3: Set $q = q + 1$. Determine the values of $\boldsymbol{X}_1^{(q)}$ and $\boldsymbol{X}_3^{(q)}$ to minimize:

$$\varepsilon_{\alpha}^{(q)} = \max_{\omega \in [\Omega_{\mathrm{p1}}, \Omega_{\mathrm{p2}}] \cup [\Omega_{\mathrm{s1}}, \Omega_{\mathrm{s2}}]} \left| W(\omega)\left[H_{\alpha}^{(q)}(\omega) - D(\omega)\right]\right|, \tag{15}$$

where

$$H_{\alpha}^{(q)}(\omega) = F^{(q)}(L\omega)G_1^{(p)}(\omega) + \left[1 - F^{(q)}(L\omega)\right]G_2^{(p)}(\omega). \tag{16}$$

In (16),

$$F^{(q)}(L\omega) = \boldsymbol{K}_1^{(q-1)}(L\omega)^{\mathrm{T}}\begin{bmatrix}\boldsymbol{X}_1^{(q)} \\ \boldsymbol{X}_3^{(q)}\end{bmatrix}, \tag{17}$$

where

$$\boldsymbol{K}_1^{(q-1)}(w) = \Bigg[1, 2\cos(\omega), \ldots, 2\cos(M\omega), 2\sum_{m=1}^{d} f^{(q-1)}(M+m)\cos((M+m)\omega), \ldots, 2\sum_{m=1}^{d} f^{(q-1)}(M+m)\cos((M+m+Rd)\omega)\Bigg]^{\mathrm{T}}. \tag{18}$$

Step 4: Set $q = q + 1$. Determine the values of $\boldsymbol{X}_1^{(q)}$ and $\boldsymbol{X}_2^{(q)}$ to minimize:

$$\varepsilon_{F}^{(q)} = \max_{\omega \in [\Omega_{\mathrm{p1}}, \Omega_{\mathrm{p2}}] \cup [\Omega_{\mathrm{s1}}, \Omega_{\mathrm{s2}}]} \left| W(\omega)\left[H_{F}^{(q)}(\omega) - D(\omega)\right]\right|, \tag{19}$$

where

$$H_{F}^{(q)}(\omega) = F^{(q)}(L\omega)G_1^{(p)}(\omega) + \left[1 - F^{(q)}(L\omega)\right]G_2^{(p)}(\omega). \tag{20}$$

In (20),

$$F^{(q)}(L\omega) = \boldsymbol{K}_2^{(q-1)}(L\omega)^{\mathrm{T}}\begin{bmatrix}\boldsymbol{X}_1^{(q)} \\ \boldsymbol{X}_2^{(q)}\end{bmatrix}, \tag{21}$$

where

$$\boldsymbol{K}_2^{(q-1)}(\omega) = \Bigg[1, 2\cos(\omega), \ldots, 2\cos(M\omega), 2\sum_{r=0}^{R} \alpha_r^{(q-1)}\cos((M+rd+1)\omega), \ldots, 2\sum_{r=0}^{R} \alpha_r^{(q-1)}\cos((M+rd+d)\omega)\Bigg]^{\mathrm{T}}. \tag{22}$$

Step 5: If $|\varepsilon_{\alpha}^{(q-1)} - \varepsilon_{\alpha}^{(q-3)}| \leqslant \Delta$ and $|\varepsilon_{F}^{(q)} - \varepsilon_{F}^{(q-2)}| \leqslant \Delta$, where Δ is a prescribed tolerance, then set

$$F^{(p)}(L\omega) = \boldsymbol{K}_2^{(q-1)}(L\omega)^{\mathrm{T}}\begin{bmatrix}\boldsymbol{X}_1^{(q)} \\ \boldsymbol{X}_2^{(q)}\end{bmatrix} \tag{23}$$

and go to Step 6. Otherwise, go to Step 3.

Step 6: If $|\varepsilon_{G}^{(p)} - \varepsilon_{G}^{(p-1)}| \leqslant \Delta$, then stop. Otherwise, go to Step 1.

Steps 1, 3 and 4 can be accomplished by using linear programming. In the above algorithm, the main idea is that the two masking filters are optimized in Step 1. The function of the two masking filter is mainly on generating the desired response on $[0,\ \Omega_{\mathrm{p1}}] \cup [\Omega_{\mathrm{s2}},\ \pi]$. The extrapolated band-edge shaping filter is optimized by iteratively adjusting the extrapolated coefficients and scaling factors, i.e., $[\boldsymbol{X}_1^{\mathrm{T}}, \boldsymbol{X}_3^{\mathrm{T}}]^{\mathrm{T}}$ and $[\boldsymbol{X}_1^{\mathrm{T}}, \boldsymbol{X}_2^{\mathrm{T}}]^{\mathrm{T}}$, respectively, in Steps 3–5. The function of the extrapolated band-edge shaping filter is mainly on generating the desired response on $[\Omega_{\mathrm{p1}},\ \Omega_{\mathrm{p2}}] \cup [\Omega_{\mathrm{s1}},\ \Omega_{\mathrm{s2}}]$. The sharing of the frequency-response-shaping responsibility was first proposed by Saramäki and Johansson [11].

5. Choosing *d* and *M*

In order to optimize the sub-filters of the proposed technique, the parameters M and d, which determine the center segment duration and

side segment durations, respectively, play important roles. In this section, choosing of the values of M and d is discussed.

As the extrapolated impulse response technique is developed from the quasi-periodic property of the impulse responses, the choosing of d is based on the observation of the impulse responses. The resemblances among the segments of impulse responses of band-edge shaping filters in FRM technique are obvious. Thus, d can be easily chosen as the duration of the side segments.

From our experiences, when M is selected to be a value close to and not less than d, the optimization procedure has high probability to produce a promising result. In actual design, the original band-edge shaping filter is obtained before the proposed optimization procedure is carried out. Therefore, the length of band-edge shaping filter, $2N_F+1$, is known, and the period of the quasi-periodicity, d, can be observed. The value of M thus may be selected in the vicinity of

$$M' = N_F - (R+1)d \tag{24}$$

experimentally by a trial and error method, where $R+1 = \lfloor \frac{N_F}{d} \rfloor - 1$.

In general, the frequency response of the overall filter incorporating extrapolated band-edge shaping filter of length $2N_F+1$ is inferior to that incorporating optimum (i.e. non-extrapolated) band-edge shaping filter (also of length $2N_F+1$). The frequency response of the filter incorporating extrapolated impulse response band-edge shaping filter may be improved by increasing the length of the extrapolated impulse response filter by appending tail coefficients.

These additional appended tail coefficients are included in, and optimized together with, the vector $\boldsymbol{X}_1^{(q)}$ shown in (14). The number of appended tail coefficient, denoted as P, usually is small and therefore is also selected experimentally. Thus, the total number of multipliers used in the extrapolated band-edge shaping filter is $d+(M+1)+2R+P$.

6. Examples

This section illustrates, by means of an example, the efficiency of the filters obtained by using the proposed techniques compared with those obtained using the earlier techniques.

Consider the specifications [11,12]: $\omega_p = 0.4\pi$, $\omega_s = 0.402\pi$, $\delta_p = 0.01$, and $\delta_s = 0.001$. For the optimum conventional direct-form FIR filter design, the minimum order to meet the given criteria is 2541, requiring 2541 adders and 1271 multipliers when the coefficient symmetry is exploited.

Using the iterative optimization approach [11], the overall number of multipliers was minimized by choosing $L = 21$. The best solution corresponds to $N_F = 61$, $N_1 = 56$ and $N_2 = 78$, where N_1 and N_2 are the filter lengths of $G_1(z)$ and $G_2(z)$. The filter requires 129 multipliers and 254 adders. The overall filter order is 2639.

It is observed that the impulse response of the band-edge shaping filter $F(z)$, obtained using the

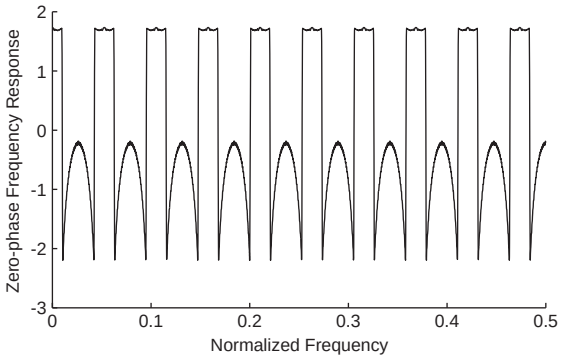

Fig. 5. Frequency response of the band-edge shaping filter, $F(z)$, with length 141, extrapolated from a filter with length 57.

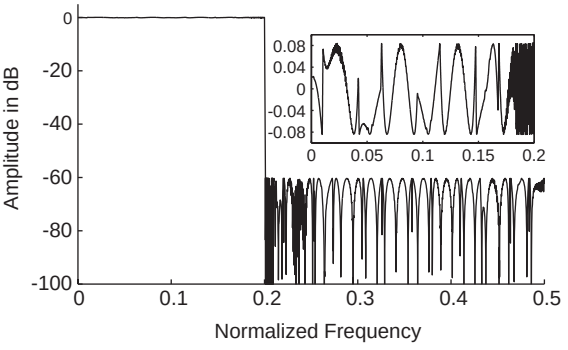

Fig. 6. Frequency response of the overall filter, in which the band-edge shaping filter with length 141 is extrapolated from a filter with length 57.

Table 1
Sub-filter coefficient values of FRM technique incorporating extrapolated impulse response band-edge shaping filter for the design where L equals to 19

n	$f(n)$	α_n	$g_1(n)$	$g_2(n)$
0	0.15933392	—	0.37754759	0.39874342
1	0.59180835	−0.47895883	0.29321608	0.30256410
2	0.48063618	0.22618556	0.10614714	0.09608974
3	−0.08736256	−0.10124625	−0.04483271	−0.05965526
4	−0.30008161	—	−0.07746582	−0.07620466
5	−0.09969006	—	−0.01969619	−0.00381350
6	0.15314345	—	0.03537029	0.04643933
7	0.16140572	—	0.03511276	0.02751208
8	−0.01584707	—	−0.00316625	−0.01858608
9	−0.13494212	—	−0.02780994	−0.03082980
10	−0.06999628	—	−0.01583009	−0.00345478
11	0.06551197	—	0.01065414	0.02156922
12	0.10080073	—	0.01948473	0.01480753
13	0.01106347	—	0.00535955	−0.00843485
14	−0.07647340	—	−0.01135053	−0.01647898
15	−0.05826126	—	−0.01053361	−0.00248023
16	0.02818759	—	0.00224031	0.01177813
17	0.06956216	—	0.01134361	0.00939716
18	0.02323268	—	0.00720553	−0.00326727
19	−0.04543308	—	−0.00064203	−0.00654340
20	−0.04930805	—	−0.00382966	0.00112585
21	0.00650186	—	0.00006183	0.00816426
22	0.04942898	—	0.00262314	0.00342301
23	0.02627201	—	0.00235411	−0.00503281
24	−0.02469745	—	—	−0.00619017
25	−0.04178573	—	—	0.00091428
26	−0.00473599	—	—	0.00563633
27	0.03238783	—	—	0.00241403
28	0.02717135	—	—	−0.00376717
29	—	—	—	−0.00493233
30	—	—	—	−0.00041079
31	—	—	—	0.00372497
32	—	—	—	0.00261179
33	—	—	—	−0.00169269
34	—	—	—	−0.00338843
35	—	—	—	−0.00088760
36	—	—	—	0.00280514
37	—	—	—	0.00340352
38	—	—	—	0.00192968
68	0.00134641	—	—	—
69	0.00736226	—	—	—
70	−0.00653259	—	—	—

iterative optimization approach [11], is quasi-periodic from $f(14)$ through $f(61)$ with period of 12, as shown by the stem plot in Fig. 4. Therefore, d is equal to 12, and M is selected to be 13 according to (24). Using the optimization procedure proposed in Section 4, the band-edge shaping filter with length 123 can be extrapolated from a filter with length of 51. However, the resulting passband and stopband ripples of the obtained overall filter are 0.018 and 0.0018, respectively.

Table 2
Comparison among the techniques mentioned in this paper

	L	d	M	R	P	Multipliers	Adders	Order
Direct form	—	—	—	—	—	1271	2541	2541
Technique proposed in [11]	21	—	—	—	—	129	254	2639
Our proposed technique	21	12	13	3	4	103	194	2807
Our proposed technique	19	13	15	3	3	101	190	2736

To meet the original specifications, an additional 8 accurately implemented coefficients appended to the impulse response, 4 at each side, may reduce the passband and stopband ripples to 0.01 and 0.001, respectively. Thirty-six multipliers and 62 adders are needed for the realization of this band-edge shaping filter when the coefficient symmetry is exploited. The overall multipliers and adders needed are 103 and 194, whereas the overall filter order is 2807.

For the proposed technique, the overall number of multipliers is minimized if the interpolation factor L is changed from 21 to 19. Using iterative optimization approach [11], an overall filter constructed by $F(z)$, $G_1(z)$ and $G_2(z)$ with $N_F = 68$, $N_1 = 47$ and $N_2 = 77$ can meet the given specification. When $F(z)$ is synthesized by extrapolated impulse response technique, d is observed to be 13 and thus M is selected to be 15 (where $M' = 16$). Furthermore, an additional three impulse responses of $f(68)$ through $f(70)$ are also realized accurately to meet the given specification. Therefore, the extrapolated band-edge shaping filter is with length 141.

The frequency response of the extrapolated band-edge shaping filter with length 141 when $L = 19$ is shown in Fig. 5. Thirty-eight multipliers and 68 adders are needed for the realization of this band-edge shaping filter when the coefficient symmetry is exploited. The overall multipliers and adders needed are 101 and 190, which are 78.3% and 74.8%, respectively, of those in the design presented in [11]. The overall filter order is 2736. Depicted in Fig. 6 is the overall frequency response. The coefficient values of the three subfilters are tabulated in Table 1. Table 2 shows the parameters used in the techniques mentioned in this paper, while all these techniques achieve the same design specification.

7. Conclusion

Extrapolated impulse response technique significantly reduces the arithmetic complexity of lowpass and highpass filters. In FRM technique, the band-edge shaping filter shows quasi-periodic property and is eminently suitable for realization using the extrapolated impulse response technique. The arithmetic complexity of FIR filters synthesized using FRM approach has been further reduced by incorporating the extrapolated impulse response band-edge shaping filter.

Acknowledgements

This project is supported in parts by Nanyang Technological University, Temasek Laboratories @ NTU, the Grant PolyU 5101/02E of the Hong Kong Polytechnic University, and a research grant from the Australian Research Council.

References

[1] Y. Lian, Complexity reduction for FRM-based FIR filters using the prefilter-equalizer technique, Circuits, Systems, Signal Processing 22 (2) (March/April 2003) 137–155.
[2] Y. Lian, A modified frequency-response masking structure for high-speed FPGA implementation of sharp FIR filters, J. Circuits, Systems, Computers 12 (5) (October 2003) 643–654.
[3] Y. Lian, Y.C. Lim, Reducing the complexity of frequency response masking filters using half band filters, Signal Processing 42 (3) (March 1995) 227–230.

[4] Y. Lian, C.Z. Yang, Complexity reduction by decoupling the masking filters from the bandedge shaping filter in the FRM technique, Circuits, Systems, Signal Processing 22 (2) (March/April 2003) 115–135.
[5] Y. Lian, L. Zhang, C.C. Ko, An improved frequency response masking approach for designing sharp FIR filters, Signal Processing 48 (81) (December 2001) 2573–2581.
[6] Y.C. Lim, Frequency-response masking approach for the synthesis of sharp linear phase digital filters, IEEE Trans. Circuits Systems CAS-33 (4) (April 1986) 357–364.
[7] Y.C. Lim, Y. Lian, The optimum design of one- and two-dimensional FIR filters using the frequency-response masking technique, IEEE Trans. Circuits Systems II 40 (2) (February 1993) 88–95.
[8] Y.C. Lim, B. Liu, Extrapolated impulse response FIR filters, IEEE Trans. Circuits Systems 37 (12) (December 1990) 1548–1551.
[9] Y.C. Lim, Y.J. Yu, H.Q. Zheng, S.W. Foo, FPGA implementation of digital filters synthesized using the frequency-response masking technique, Circuits, Systems Signal Processing 22 (2) (March/April 2003) 211–218.
[10] W.S. Lu, T. Hinamoto, Optimal design of frequency-response-masking filters using semidefinite programming, IEEE Trans. Circuits Systems I 50 (4) (April 2003) 557–568.
[11] T. Saramäki, H. Johansson, Optimization of FIR filters using the frequency-response masking technique, Proceedings of the IEEE International Conference on Circuits Systems, Sydney, Australia, May 2001, vol. II, pp. 177–180.
[12] T. Saramäki, Y.C. Lim, Use of the Remez algorithm for designing FRM based FIR filters, Circuits, Systems, Signal Processing 22 (2) (March/April 2003) 77–97.
[13] T. Saramäki, J. Yli-Kaakinnen, Optimization of frequency-response-masking based FIR filters with reduced complexity, Proceedings of the IEEE International Conference on Circuits Systems, Phoenix, AZ, May 2002, vol. 3, pp. 26–29.
[14] Y.J. Yu, Y.C. Lim, FRM based FIR filter design—WLS approach, Proceedings of the IEEE International Conference on Circuits Systems, Phoenix, AZ, May 2002, vol. 3, pp. 221–224.